“Capacity analysis of underwater acoustic MIMO communications”

A THESIS SUBMITTED FOR PARTIAL FULFILLMENT OF THE REQUIREMENTS FOR THE DEGREE OF

Bachelor of Technology

In

Electronics and Communication Engineering

Under the guidance of **Prof. Poonam Singh**

Completed by:

Sunil Gautam Panda (108EC003)

Birupaksha Bhattacharjee (108EC031)

National Institute of Technology, Rourkela

2008-2012

CERTIFICATE

This is to certify that the thesis entitled "**Capacity analysis of underwater acoustic MIMO communications**" submitted by **Mr. Sunil Gautam Panda** and **Mr. Birupaksha Bhattacharjee** for partial fulfilment for the requirement of Bachelor in Technology degree in **Electronics and Communication Engineering** at National Institute of Technology, Rourkela is an authentic piece of work carried out by them under my guidance and supervision.

To the best of my knowledge, the matter in this thesis has not been submitted to any other University / Institute for the award of any Degree.

Prof. Poonam Singh

Department of Electronics and Communication

National Institute of Technology, Rourkela

Date:

ACKNOWLEDGEMENT

It would not have been possible to complete and write this project thesis without the help and encouragement of certain people whom we would like to deeply honour and value their gratefulness.

We would like to highly appreciate the constant motivation and encouragement shown by our supervisor and guide **Prof. Poonam Singh**, Department of Electronics and Communication Engineering during the project and writing of the thesis. Without her guidance and help, it would not have been possible to bring out this thesis and complete the project.

We also express our gratitude towards **Dr. Sukadev Meher** , HOD, Department of Electronics and Communication, for his selfless support and help offered whenever needed, especially for the usage of laboratories. Other professors of the department equally have a space for respect in this thesis for their support.

Last but not the least, our sincere thanks to all the friends who have directly or indirectly helped us in all the respect regarding the thesis and project. Also, we are indebted to our institute, NIT Rourkela to have provided the platform for gaining the precious knowledge and framing the paths of glory for our future.

SUNIL GAUTAM PANDA

108EC003

BIRUPAKSHA BHATTACHARJEE

108EC031

Contents

ABSTRACT

Multi-Input Multi-Output (MIMO) principle is based on transmitting digital data from *Nt* transmitters to *Nr* receivers within a frequency band. In the last decade, theoretical works and practical experiments in wireless and cellular networks have convincingly proved that MIMO has been a real find in digital communications.

Nowadays, MIMO principle is being applied to underwater acoustic communications (UAC) and it is showing encouraging results. But very few research has been done on the relation between different parameters of MIMO and its gain. Our primary purpose in this project is to analyse the MIMO gain theoretically using Shannon capacity analysis and suggest ways to maximize capacity with limited bandwidth by varying other parameters .

As we will show in the later pages of this project that underwater acoustic channel (UAC) is highly selective in frequency, data transmission cannot be increased by simply increasing the transmission bandwidth. This difficult situation can be found in wireless communication where there is an increasingly large requirement in high speed data transfer but available bandwidth is constrained by the frequency allocation law. In those communication fields where radio frequency is used , this bandwidth limitation problem has been overcome by introducing MIMO techniques, which provide significant gain in data transmission rate while keeping the transmission Bandwidth constant.

In the previous years, the contribution of MIMO to UAC systems has mostly been thoroughly analyzed via spatial modulation or multi-carrier modulation. Initial simulation and experimental results have showcased a larger gain over conventional single input single output (SISO) but the results strongly vary depending on the modulation scheme chosen by us and the receiver algorithm as well as the underwater channel environment.

List of figures

List of Tables

INTRODUCTION TO MIMO COMMUNICATIONS

The channel capacity computed according to Shannon's theorem represents the tightest upper bound on the volume of information that we can reliably transmit over a data communications channel. Therefore the channel capacity of the available channel is the limiting information rate (having the unit of information per unit time) that we can achieve with relatively small error probability regardless of the algorithm used in the receiver unit.

While research is being carried out extensively on assessing capacity of wireless radio transmission, relatively fewer analysis have been done, that too focusing on SISO channel. The few available references that are dealing with MIMO underwater acoustic capacity provide capacity estimation using simulation and through the use of experimental data, but under the common assumption that a transmitter has knowledge of the channel transfer function which is not practically possible in Underwater Acoustic Channel(UAC).The purpose of our project is to provide extensive theoretical analysis of the MIMO underwater capacity under the supposition of shallow water acoustic (SWA) channel by taking into consideration both the underwater propagation and, multi-path bandwidth limitation to give an approximate result of theoretically maximum data rate expected from a real-time MIMO UAC system.

When compared to radar propagation(EMW) through the atmosphere, underwater acoustic propagation is highly characterized by frequency dependent disturbances and relatively slower speed of propagation. In addition to the above

,transmission loss and noise also form principal factors in determining the functional vicinity of underwater communication system. Still the slow speed of wave propagation leads to time-varying multipath phenomenon which results in multipath fading. Hence this also has an influence in system design and normally imposes severe limitations on the performance of the system.

MOTIVATION AND CHALLENGES

First introduced during world war II especially for military needs, underwater communications today have a growing need in a number of civil and commercial applications like remote control in off-shore oil industry, monitoring pollution in environmental systems, efficient collection of scientific data recorded at stations located at sea bed, communication among divers as well as underwater vehicles and mapping of the sea bed for detecting objects as well as for the discovering new resources.

As we all know that electromagnetic waves cannot propagate over long distances in seawater because of high dielectric constant, underwater acoustic has become the core enabling technology for these applications. However underwater acoustic channel shortcomings such as signal fading, multi-path bandwidth limitations also known as reverberation pose very tough challenges for the development of effective underwater acoustic channel(UAC) systems. But on the other hand, data transmission rate required for UAC applications is continuously surging with the arrival of high quality images, real-time videos and the deployment of autonomous underwater networks like ad-hoc deployable sensor networks or/and autonomous fleets of cooperating unmanned under-ocean vehicles (UUV).

4. CHANNEL CHARACTERISTICS

When compared to electromagnetic propagation that flows through the atmosphere, underwater acoustic signals' propagation is characterized significantly by frequency causing disturbances and relatively quite slower speed of propagation. Transmission loss and noise also contribute to the principal factors that determine the functional point of a underwater communication system, but the slow speed of the propagating wave leads to time-varying multipath phenomenon that also has a say in the system design and generally imposes severe limitations on the performance of the system.

4.1 Transmission loss

The attenuation mechanisms that impacts underwater acoustic signal can be viewed principally as the sum of these three terms : the spreading loss, absorption loss and reflection loss. The spreading losses are due to the flow and hence the expansion of the fixed amount of transmitted energy over a larger area as the signal slowly propagates away from its source. It is already proved that the energy decays at a rate of l^$(-k)$ where l is the distance and k is the spreading factor depending upon the geometry of propagation (its commonly used values are $k = 2$ for spherical spreading, $k = 1$ for cylindrical spreading and $k = 1.5$ for all practical spreading).

The second mechanism of the transmitted signal's power loss, called absorption loss, results from the conversion of energy of the propagating wave into heat. In case of under-ocean acoustic transmission, the absorption loss is directly linked to the wave frequency, such that the signal energy/power decay due to absorption loss is proportional to $\exp(-\alpha(f)l)$ where

$\alpha(f)$ (referred as the absorption coefficient) is an increasing function of frequency. The absorption loss can be expressed empirically using the Thorp's formula which gives $\alpha(f)$ (in dB/km) for frequency f (in kHz)

$$10\log\alpha(f) = 0.11\frac{f^2}{1+f^2} + 44\frac{f^2}{4100+f^2} + 2.75\cdot 10^{-4}f^2 + 0.003 \tag{1}$$

This formula is valid for $f > 400$ kHz. For lower frequencies, the formula becomes:

$$10\log\alpha(f) = 0.002 + 0.11\frac{f^2}{1+f^2} + 0.011f^2 \tag{2}$$

By hitting the sea-surface, sea-bed or another under-sea object, the sound wave is partially or totally reflected depending on the wave frequency, the sound speed and the type of obstacle. The reflection loss suffered along path p is denoted as Γp and will be described more in depth.

As a result, the total path loss that occurs in a under-ocean acoustic channel can be computed by the equation:

$$\frac{\Gamma_P}{\sqrt{A(l,f)}}$$

where $A(l, f)$ is the sum of spreading and absorption loss:

$$10\log A(l,f) = k\cdot 10\log l + l\cdot 10\log\alpha(f) \tag{3}$$

4.2. Noises

There are several natural sources of ambient noise in the ocean in the range of frequencies of interest for acoustic communications. Usually these four sources are considered: turbulence, shipping, waves and thermal noise. They can be modeled by a coloured Gaussian noise with the empirical power spectral density (p.s.d.) given in dB , μ per Hz as a function of frequency (in kHz) :

$$10 \log Nt(f) = 17 - 30 \log f$$

$$10 \log Ns(f) = 40 + 20(s - 0.5) + 26 \log f - 60 \log(f + 0.03)$$

$$10 \log Nw(f) = 50+7.5w1/2 + 20 \log f - 40 \log(f + 0.4)$$

$$10 \log Nth(f) = -15 + 20 \log f$$

where s is the shipping activity whose value always ranges from 0 to 1 for low and high activity respectively, w is the wind speed expressed in m/s. The overall p.s.d. of the ambient noise is noted $N(f)$ and expressed as the sum of the four above mentioned noise components:

$$N(f) = Nt(f) + Ns(f) + Nw(f) + Nth(f) \tag{4}$$

This strong dependency of the ambient noise on frequency is one of major factor we have to consider when selecting frequency bands for underwater acoustics transmission.

4.3. Multi-paths propagation

In most environments and in range of frequency of interest for communications signals, the underwater channel results in paths of multiple propagation from each source to receiver.

The multi-paths spread depends in the transmission link configuration designed as horizontal or vertical. While vertical links have less time dispersion, horizontal channels exhibit a relatively long delay spread. Mechanism of multi-paths formation are also strongly dependent on the ocean depth: in case of high depth, multi-paths are formed by ray bending which occurs as the sound waves tend to reach region of lower propagation speed while in case of shallow water environment, multi-path mechanism results due to reflections on surface bottom bounces and/or a possible direct path. The definition of shallow and deep water is not a rigid one, but it is generally assumed that shallow water stands for a water depth less than 100 m

Moreover we have assumed a constant water temperature within the whole water depth which is important because a constant temperature gives a constant sound speed (iso velocity).

In a digital communication system, multi-paths propagation causes inter-symbol interference (ISI) and also multi path fading that have to be carefully treated with a equaliser at the receiver side in order to get an acceptable SNR(signal to noise ratio).

As result, the design of underwater communication systems is aided and approximated through the use of propagation model for predicting the multi-path propagation. Ray theory and the other theories of such normal modes provide basis for such propagation modelling.

At high frequencies, ray tracing gives an appropriate approximation and is commonly used to determine the dense multi-paths design of the channel. We will consider medium range transmission (range$\leq$ 5 km) which generally requires high frequency and justifies the use of ray model as the basis of channel propagation model.

4.4. Time-variation

Each and every propagation path may also be characterized by a random varying component which results due to the scattering on moving sea-surface (waves or bubbles). Motion of the reflection surfaces result in the Doppler spreading of the reflected signals leading to a transient impulse response of the channel which is time varying. We can note that time-varying effect is omnipresent within the underwater channel regardless of an eventual motion of transmitter or receiver. For the sake of simplicity, we'll assume in our study a calm sea-surface so that surface scattered paths in the impulse response are both enough stable and localized in delay.

5. MIMO CHANNEL MODEL

In this section we first design a mathematical model for signal propagation through a SWA (shallow water acoustics) channel based on ray tracing model derived from ocean physics. Then we have tried to design a filter-based representation of the channel and finally we have tried to extend this model into MIMO structure design.

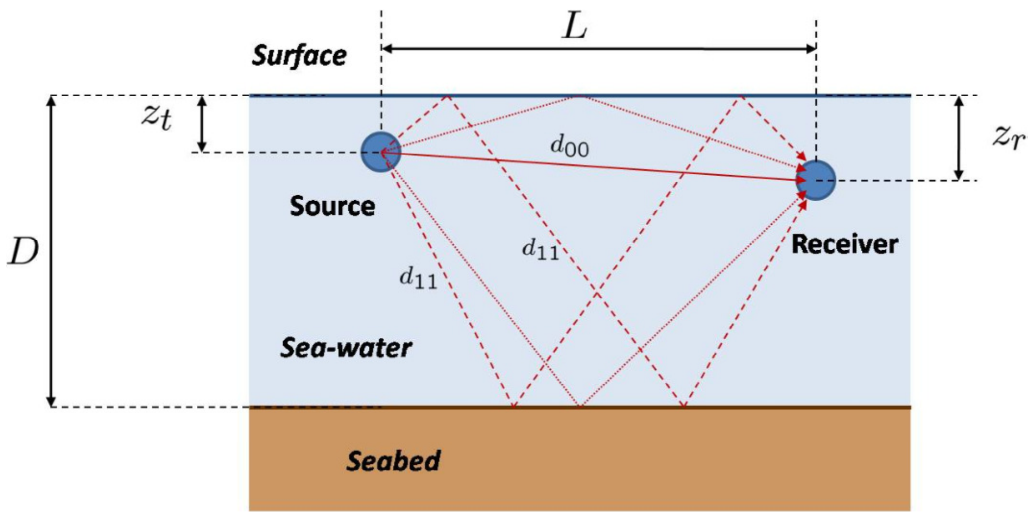

Fig. 5.1. SISO Channel representation

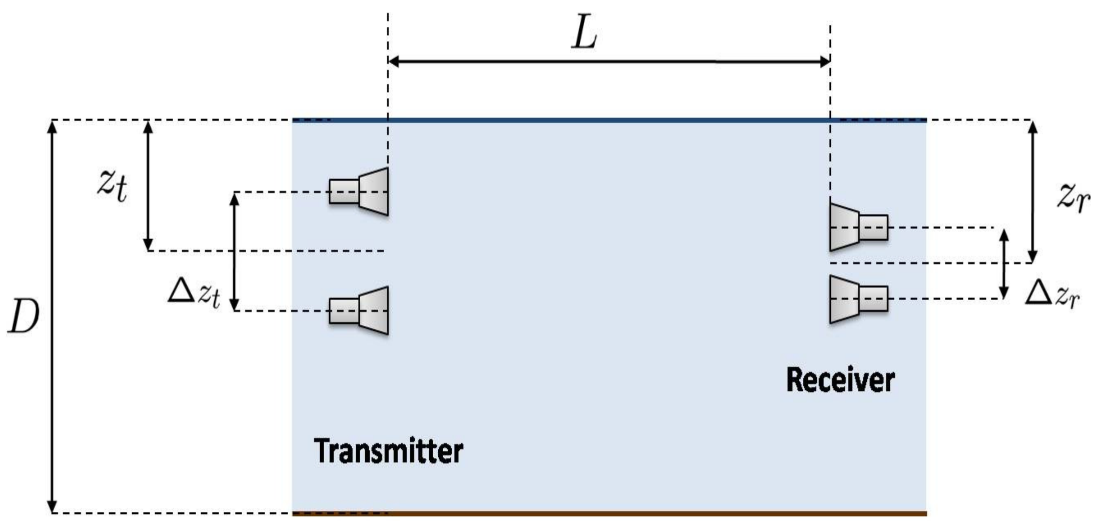

Fig. 5.2. MIMO SWA Channel representation

5.1 Propagation model based on ray tracing

In the ray propagation model which we have used, sound energy is assumed to propagate along *rays*, which are almost straight lines in the case of liquid medium with constant sound speed (isovelocity at constant temperature). They are partially reflected and refracted when they confront a discontinuity in sound speed.

We model the SWA channel like a wave guide consisting of an isovelocity layer (the ocean water) between two isovelocity half spaces: air and ocean-bed. The isovelocity assumption is justified as shallow water channel are generally well mixed and very small increase in pressure as we go deeper into the water/ocean.

Let us assume *L* to be the transmission range, *D* the water depth, *zt* and *zr* to be the depth of the transmitter and the receiver respectively. The distance travelled by the sound along various rays can be calculated using the geometrical approach. Let *dsb* be the distance along an upward originating eigen ray with *s* surface reflections and *b* bottom(sea-bed) reflections. The distance along a direct ray *d*00 can be computed according to the equation:

$$d_{00} = \sqrt{R^2 + (z_t - z_r)^2} \tag{5}$$

In the general case, if $0 \leq s - b \leq 1$, the distance becomes

$$d_{sb} = \sqrt{R^2 + (2bD + z_t - (-1)^{s-b} z_r)^2} \tag{6}$$

Inversely, if $0 \leq b - s \leq 1$, we have:

$$d_{sb} = \sqrt{R^2 + (2bD - z_t + (-1)^{b-s} z_r)^2} \quad (7)$$

Attenuation coefficient due to reflections on the surface only is denoted Γ+ and is relatively small in magnitude because of the impedance mismatch between the seawater and air. If the sea is calm and still with no turbulence, reflection coefficient generally tends to perfect reflection value 1. But if the sea surface is rough (due to waves), a loss would be incurred for every surface interaction. Let this loss be modelled by a constant coefficient *LSS*. On the ocean-bed that is the bottom, the coefficient reflection varies according to the impedance variation. Such coefficient estimation can be obtained using Rayleigh reflexion law:

$$\Gamma^- = \left| \frac{\frac{\rho_1}{\rho}\cos\theta - \sqrt{(c/c_1)^2 - \sin^2\theta}}{\frac{\rho_1}{\rho}\cos\theta + \sqrt{(c/c_1)^2 - \sin^2\theta}} \right| \quad (8)$$

where ρ and $\rho 1$ are density of water and ocean-bed respectively, c and $c1$ are sound speed in water and ocean-bed respectively while θ is the angle of incidence of the reflected wave that can be computed from the ray dsb by the following equation, if $0 \leq s - b \leq 1$ [21]:

$$\theta_{sb} = \tan^{-1}\left(\frac{L}{2bD + z_t - (-1)^{s-b} z_r}\right) \quad (9)$$

and if $0 \leq b - s \leq 1$:

$$\theta_{sb} = \tan^{-1}\left(\frac{L}{2bD - z_t + (-1)^{b-s} z_r}\right) \tag{10}$$

Additional reflection losses due to rough or absorbing sea bottom is modeled by a constant coefficient *LSB*. Finally the total reflection loss for a path with *s* surface and *b* bottom reflections is equal to:

$$\Gamma_{sb} = (\Gamma^{+} \cdot L_{SS})^{s} \cdot (\Gamma^{-} \cdot L_{SB})^{b} \tag{11}$$

The arrival time of each ray τsb is easily computed from the distance along the ray and sound speed:

$$\tau_{sb} = \frac{d_{sb}}{c} \tag{12}$$

5.2 FIR tap representation

By traveling from a transmitter to a receiver, every ray follows a path of length *dsb* with time of arrival *τsb* and an attenuation of

$$\Gamma_{sb} / \sqrt{A(d_{sb}, f)}$$

The SWA channel is modelled by taking into account all the paths possible and they result in a Finite Impulse Response (FIR) filter with transfer function as shown:

$$\begin{aligned} H(f) &= \frac{1}{\sqrt{A(d_{00}, f)}} e^{-j2\pi f \tau_{00}} \\ &+ \sum_{s=1}^{+\infty} \sum_{b=s-1}^{s} \frac{\Gamma_{sb}}{\sqrt{A(d_{sb}, f)}} e^{-j2\pi f \tau_{sb}} \\ &+ \sum_{b=1}^{+\infty} \sum_{s=b-1}^{b} \frac{\Gamma_{sb}}{\sqrt{A(d_{sb}, f)}} e^{-j2\pi f \tau_{sb}} \end{aligned}$$

For practical computation, we'll assume that number of reflections on surface and sea-bottom is finite and equal to *smax* and *bmax* respectively. Total number of paths is then equal to *P* with:

$$P = 1 + 2s_{\max} + 2b_{\max} \tag{13}$$

The channel transfer function can be rewritten as a closed from expression:

$$H(f) = \sum_{p=0}^{P-1} \frac{\Gamma_P}{\sqrt{A(l_p, f)}} e^{-j2\pi f \tau_p} \tag{14}$$

Where Γp , *A*(*dp*) and *τp* are the total reflection loss, the medium attenuation, and the time taken to arrive at the receiver along path *p* respectively.

5.3. Extension to MIMO

We now consider a MIMO underwater channel structure with Nt transmitter hydrophones and *Nr* receiver hydrophones. On the transmitter and receiver sides, each hydrophone pair has a constant vertical separation of Δ*zt* and Δ*rt* respectively. The transmitter and receiver depths *zt* and *zr,* as shown in figure 2, correspond to the middle of each array. The MIMO array is placed in vertical direction so as to maximize the delay spread difference between each sub-channel and thus minimize the resulting spatial correlation.

The MIMO channel is hereby modelled by *Nt* × *Nr* sub-channels, where each sub-channel corresponds to the SWA channel model as thoroughly explained in the previous section. As a result, the transfer function of sub-channel connecting hydrophone *m* ∈ [1,*Nt*] to hydrophone *n* ∈ [1,*Nr*] denoted *Hmn*(*f*) can be derived from the following equation :

$$H_{mn}(f) = \sum_{p=0}^{P-1} \frac{\Gamma_P}{\sqrt{A(d_{p,mn}, f)}} e^{-j2\pi f \tau_{p,mn}} \qquad (15)$$

where *dp,mn* is the distance of thw signal transmission along the *p*-th path of sub-channel *mn* and *τp,mn = dp,mn/c*. In order to analyse the geometry of the MIMO array, each distance *dp,mn* is computed by *zt* and *zr* by *ztm* and *zrn* respectively in the above equations such as:

$$z_t \to z_{tm} = z_t - (N_t + 1 - 2m)\frac{\Delta z_t}{2} \qquad (16)$$

$$z_t \to z_{rn} = z_r - (N_r + 1 - 2n)\frac{\Delta z_r}{2} \qquad (17)$$

Hence now, the whole MIMO channel is represented by the following $Nt \times Nr$ channel matrix:

$$H(f) = \left[\begin{pmatrix} H_{11}(f) & \dots & H_{N_t 1}(f) \\ \vdots & \ddots & \vdots \\ H_{1N_r}(f) & \cdots & H_{N_t N_r}(f) \end{pmatrix} \right]_{N_r \times N_t} \tag{18}$$

6 CAPACITY COMPUTATION

The SHANNON channel capacity gives the maximum data transmission rate that can be reliably transmitted through a communications channel. This quantity is defined as the maximum of the average mutual information $I(\mathbf{x}, \mathbf{y})$ between a input signal **x** and its corresponding output signal **y** of the channel over a choice of distribution of **x**. As shown in the following, we determine the capacity formula of SWA MIMO channel by taking into account all the relations derived in section II earlier. In order to determine the SWA MIMO capacity, we also get a idea of useful capacity bounds both for SISO and MIMO transmission channel.

6.1 SWA MIMO Channel

In case of deterministic MIMO, E. Telatar derived the general expression for MIMO capacity:

$$C(f) = \log_2(I_{N_t} + \frac{S(f)}{N_t * N(f)} H(f) R_{SS} H(f)^H) \tag{19}$$

where $\mathbf{I}Nt$ is the $Nt \times Nt$ identity matrix, *SNR* is the signal-to-noise ratio, **H** is MIMO matrix(FIR), **Rss** is the covariance matrix of input signal and *H'* denotes the transpose conjugate operand of H. As demonstrated by C. E. Shannon in the SISO case, E. Telatar did the similar representation, that mutual information is maximized by choosing input signal vector **s** as an independent one and zero mean Gaussian samples [5].

Let λi be the eigen values of **H** with $0 \leq i < r$ where r = rank (**H**), the above expression can be expanded as:

$$C = \sum_{i=0}^{r-1} (1 + \frac{SNR}{N_t} \lambda_i) \tag{20}$$

Since the right part of the above expression is similar to a SISO capacity, hence the MIMO capacity can be viewed as a sum of r SISO capacities. The MIMO capacity is thus seen to be maximized when rank of **H** reaches its maximum value which can be shown to be equal to max(r) = min(Nt,Nr). This leads to a very popular realtion of MIMO system: at its best MIMO capacity gain is increasing linearly with minimum number of transmitter and receiver sensors. And in general, advantages of MIMO depends on matrix **H**, the larger the rank and eigenvalues **HH'** have, the more MIMO capacity we can generate. If the channel characteristics at the transmitter side could be known (for example through a feedback loop), capacity can be maximized by adjusting the covariance matrix *RSS* of the transmitter signal with water-filling technique. But in UWA communications, the high variability and latency of the channel makes it difficult to have any feedback from receiver to transmitter and therefore the channel matrix is usually assumed as unknown for the transmitter. In the absence of channel state information at the transmitter it is quite reasonable to choose the transmit signal **s** as white in space and in frequency spatial directions: **Rss** = **I***Nt* . Therefore the total transmit power *Ps* can be assumed to be uniformly distributed over the bandwidth *B* such as the power profile density (p.s.d.) of a signal transmitted from hydrophone $m \in [1, Nt]$ is expressed as:

$$S(f) = \frac{P_S}{B * N_t}, \forall f \in \left[f_0 - \frac{B}{2}, f_0 + \frac{B}{2} \right] \tag{21}$$

where $f0$ is central carrier frequency around which the signals are transmitted. At the receiver side, the total power received from hydrophone $n \in [1,Nr]$ is equal to:

$$P_{R_n} = \int_{f_0-\frac{B}{2}}^{f_0-\frac{B}{2}} R_n(f)df \qquad (22)$$

where Rn is the received signal p.s.d. viewed by hydrophone 'n':

$$R_n(f) = \sum_{m=1}^{N_t} |H_{mn}(f)|^2 \, S(f) \qquad (23)$$

On the other hand, the total noise power is:

$$P_N = \int_{f_0-\frac{B}{2}}^{f_0+\frac{B}{2}} N(f)df \qquad (24)$$

As a result the the signal-to-noise ratio that is viewed at receive hydrophone $n \in [1,Nr]$ can be computed by:

$$SNR_n = \frac{P_{R_n}}{P_N} \qquad (25)$$

whereas the SNR p.s.d. is:

$$SNR_n(f) = \frac{R_n(f)}{N(f)} \qquad (26)$$

Previous capacity formulas were calculated under the assumption that MIMO channel defined and characterised by matrix **H** is flat fading. Let now consider a tone f within the tavailable bandwidth for which the SWA channel can be considered flat, then formula (19) can be rewritten as shown:

$$C(f) = \log_2(I_{N_t} + \frac{S(f)}{N_t * N(f)} H(f)H(f)^H) \tag{27}$$

where $N(f)$ is the underwater noise power spectral density (p.s.d.) described in section II whereas $\mathbf{H}(f)$ is the shallow water acoustics (SWA) channel transfer function introduced in section III. The total channel capacity can be obtained by integrating $C(f)$ over the bandwidth B as below:

$$C(f) = \int_{f_0 - \frac{B}{2}}^{f_0 + \frac{B}{2}} C(f) df [bits / s / hz] \tag{28}$$

6.2 SWA SISO Channel

The Shannon capacity of a SWA SISO channel is obtained by assuming the above equations to be a single hydrophone case i.e. Nt = 1 and Nr = 1 which leads to the to the following equation:

$$C_0 = \int_{f_0-\frac{B}{2}}^{f_0+\frac{B}{2}} \log_2(1+\frac{S_0(f)}{N(f)}|H_{11}(f)|^2)df \tag{29}$$

where the power spectral density (p.s.d). of the transmitted signal becomes:

$$S_0(f) = \frac{P_S}{B}, \forall f \in \left[f_0 - \frac{B}{2}, f_0 + \frac{B}{2} \right] \tag{30}$$

6.3 Upper Bounds

In the absence of channel characteristics' knowledge at the transmitter side as described above, capacity of an arbitrary SISO channel can be shown to be bounded by a so called AWGN capacity obtained over a memory less additive white Gaussian noise (AWGN) channel and computed according to the following:

$$\overline{C}_0 = \log_2(1+\frac{P_S}{P_N})[bits / s / hz] \qquad (31)$$

By using (20) and (31), we can show that the capacity of an arbitrary MIMO channel is bounded by:

$$\overline{C} = \min(N_t, N_r) * \log_2(1+\frac{P_S}{P_N})[bits / s / hz] \qquad (32)$$

This result can be interpreted as the optimum MIMO scheme which is equivalent to min (*Nt,Nr*) AWGN channels at separate bandwidths.

6.4. Rayleigh bounds

In wireless communications, a usual channel model consists of frequency fading modelling as i.i.d. random Rayleigh coefficients. Each channel coefficient i.e. *hmn* of matrix **H** can be modelled as uncorrelated complex Gaussian samples with mean equal to zero and variance equal to unity. Channel capacity is computed by taking the expectation of instantaneous capacity over the realization of **H**:

$$C(f) = \varepsilon_H[\log_2(I_{N_t} + \frac{P_S}{N_t P_N} HH^H)][bits/s/hz] \tag{33}$$

Such capacity is called ergodic since it is assumed that the channel transfer function obeys an ergodic(positive recurrent aperiodic state of stochastic systems) random process. As stated previously, the equivalent SISO capacity is obtained by mapping to the single hydrophone case:

$$\tilde{C}_0 = \varepsilon_{h_{00}}[\log_2(I_{N_t} + \frac{P_S}{N_t P_N} | h_{11} |^2)][bits/s/hz] \tag{34}$$

TABLE I

SIMULATION PARAMETERS

LETTER	NAME	DEFAULT VALUE
F_0	Carrier Frequency	32 KHz
B	Signal Bandwidth	12 KHz(variable)
F_S	Sampling Frequency	500 KHz
Δf	Frequency resolution	7.6 Hz
L	Range	1500 m (variable)
D	Water depth	20 m (variable)
Nt	Number on transmit hydrophones	2
Nr	Number on receive hydrophones	2
zt	Transmit array depth	9 m
Δzt	Vertical separation of transmit array	0.6 m (variable)
zr	Receive array depth	9 m

Δzr	Vertical separation of receive array	0.6 m(variable)
k	Spreading factor	1.5
c	Sound speed in water	1500 m/s
ρ	Water density	1023 kg/m3
$c1$	Sound speed in sea-bottom	1650 m/s
$\rho1$	Sea-bottom density	1500 kg/m3
LSS	Absorption loss at sea-surface	–0.5 dB
LSB	Absorption loss at sea-bottom	–3 dB

7. SIMULATION RESULTS AND DISCUSSIONS

7.1 Channel Transfer function as a function of frequency

The figure below shows the channel transfer function (h(f)) as a function of frequency. The value of the response decreases as the frequency is increased .Thereby exhibiting the fact that the transfer function is dependent on $A(l, f)$.

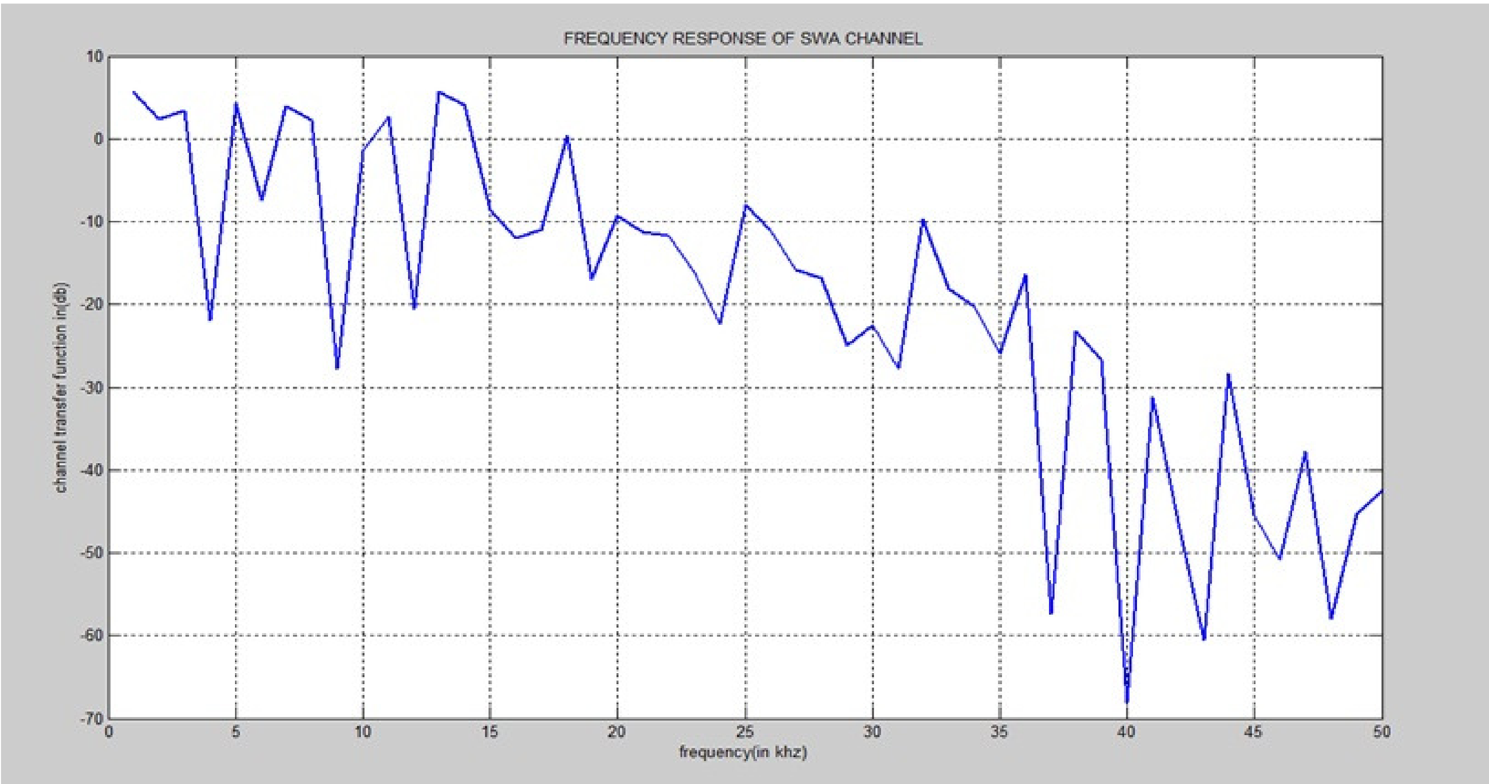

Fig. 7.1. Example of frequency response of SWA channel

Discussion

1. While traveling from transmitter to receiver, each ray of the signal follows a path of length dsb having an arrival time of τsb and an attenuation of Γsb/A(dsb, f).
2. The SWA channel is modeled by taking into account all possible paths and gives rise to a Finite Impulse Response (FIR) filter with following transfer function

$$H(f) = \sum_{p=0}^{P-1} \frac{\Gamma_P}{\sqrt{A(l_p, f)}} e^{-j2\pi f \tau_p}$$

7.2 Capacity of the SWA MIMO channel

Figure OUTPUT 2 shows the 2 X 2 MIMO capacity (*C*) and SISO capacity (*C*0) results of a SWA channel by using the default parameters depicted in table I.

To begin with, we can observe that the capacity gain is larger for the MIMO architecture as compared to the SISO architecture. As an example for *SNR* = 15 dB, SWA channel capacity for the SISO is about 3.9 bits/s/Hz while for MIMO it is foubd to be around 8 bits/s/Hz. Thus it represents a maximum MIMO data transmission rate of 96 kbits/s with the chosen bandwidth of 12 kHz. Therefore it clearly shows that the MIMO gain is about 103 % more than SISO gain thus exhibiting that the SWA capacity is increasing linearly with min(*Nt,Nr*) .

As a consequence, larger gains could be achieved by increasing the number of hydrophones in the transmitter and receiver side.

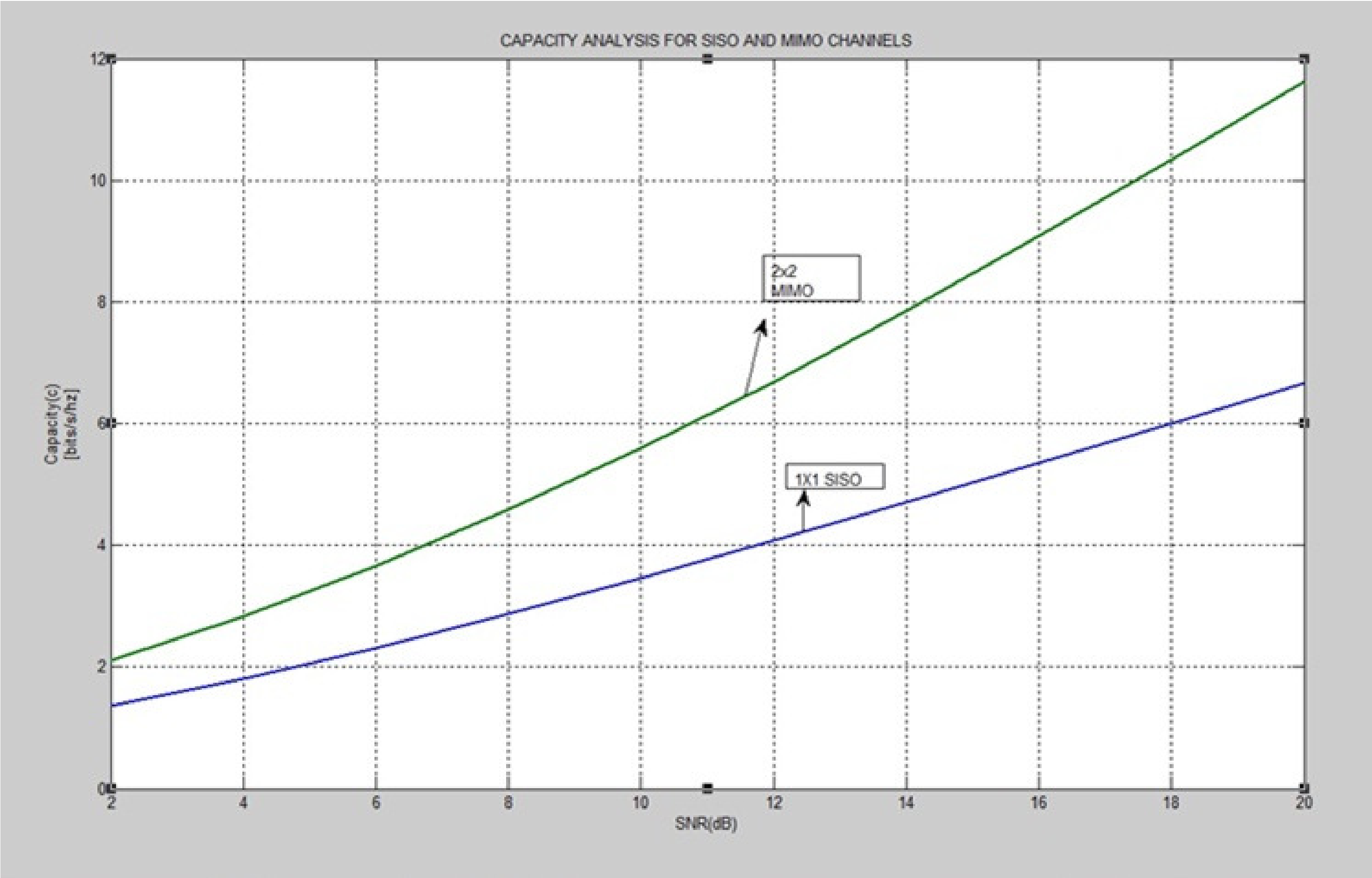

fig. 7.2. MIMO 2 × 2 and SISO capacities as function of *SNR*. Default parameters are set for SWA channel model.

Discussion

1. We can observe the increase in capacity gain brought about by the MIMO architecture.
2. The MIMO gain is found to be about 103 % higher than the SISO gain thus showcasing that the SWA capacity is increasing linearly with min(*Nt,Nr)*.
3. Even greater capacities could be accomplished by increasing the number of hydrophones both at the transmitter and receiver sides.

7.3 Bandwidth and communication range

7.3.1 SNR(f) VS frequency for different values of communication range D.

The figure below plots SNR(f) as a function of frequency for different values of communication range D.

As described earlier, sound wave propagation in water is extremely sensitive to the wave frequency. This dependency of SNR(f) on frequency is illustrated by the fact that *SNR*(*f*) includes on the one hand a frequency dependent term represented by the quantity *A*(*l, f*)*N*(*f*) also referred to as the *AN* product and on the other hand a frequency fading coefficient represented by the term $\exp(-j2\pi f\tau p)$.

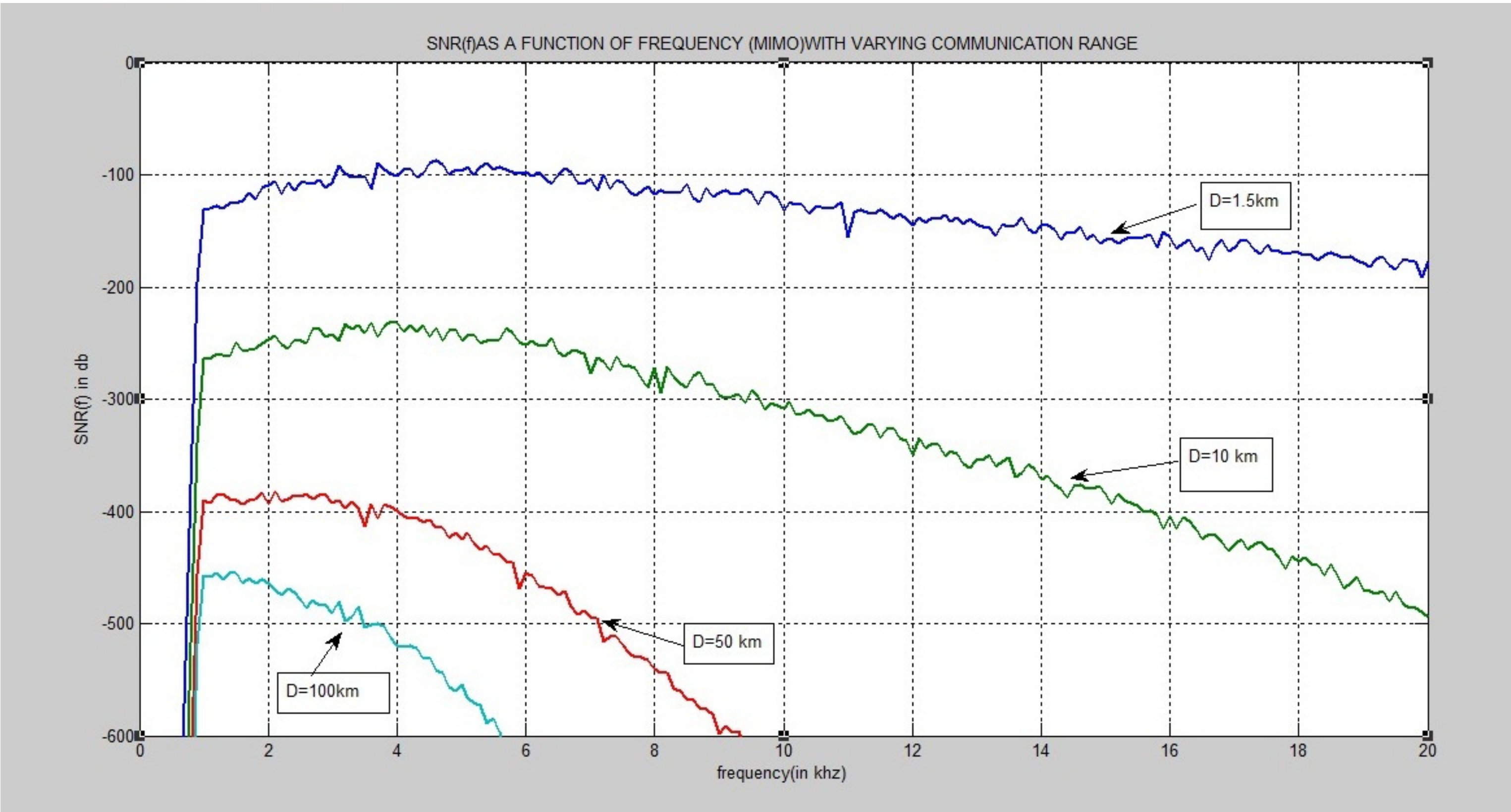

Fig. 7.3. *SNR*(*f*) at output of 2×2 SWA channel as a function of frequency

Discussion.

1) In the MIMO configuration, the reliance of SNR(f) on frequency is exemplified in figure OUTPUT 3

2) As observed in the SISO case, SNR becomes increasingly frequency selective when communication range D is increased henceforth leading to a smaller bandwidth usable for the purpose of data transmission.

3) Furthermore it is observed that, operating frequencies are decreasing for long range values of D indicating that high frequencies are dedicated to small or medium range communications

.

4) We also notice that SNR becomes more smoother as communication range increases, demonstrating that for longer ranges, the dominant factor is not the frequency fading but the transmission loss which is represented by the *AN* product.

7.3.2 Capacity vs Communication range

The underlying figure shows MIMO and SISO capacities as function of communication range *D* for a fixed *SNR* of 15 dB.

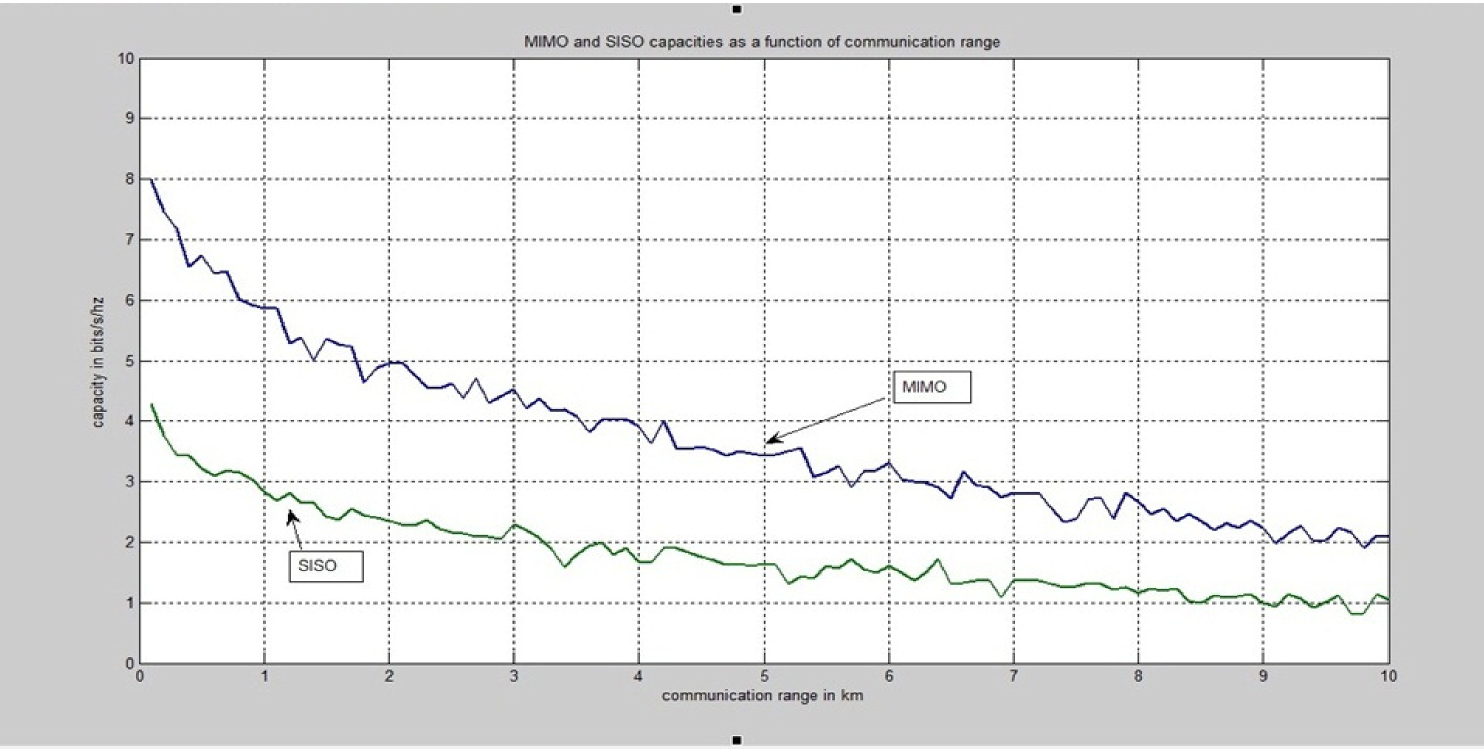

Fig. 7.4. MIMO and SISO Capacities as function of communication range

Discussion

1. The above graph shows that both SISO and MIMO SWA capacities decrease when the value of communication range D increases.
2. The above stated phenomenon is a definitive feature that distinguishes an underwater acoustic system from a terrestrial radio communication system: UAC capacity is strongly dependent on the transmission distance .
3. Nonetheless one can observe that MIMO SWA capacity fades more rapidly than the SISO SWA capacity thus indicating that the frequencies to be used in MIMO transmission have to be carefully selected as a function of the desired communication range.

7.4. Influence of water depth

Figure OUTPUT 5 shows the MIMO and SISO capacity results for varying values of water depth *D*. We can observe that MIMO capacity gain is slowly decreasing with an increase is water column depth. The largest gain is observed for very shallow water (≤ 30 m).

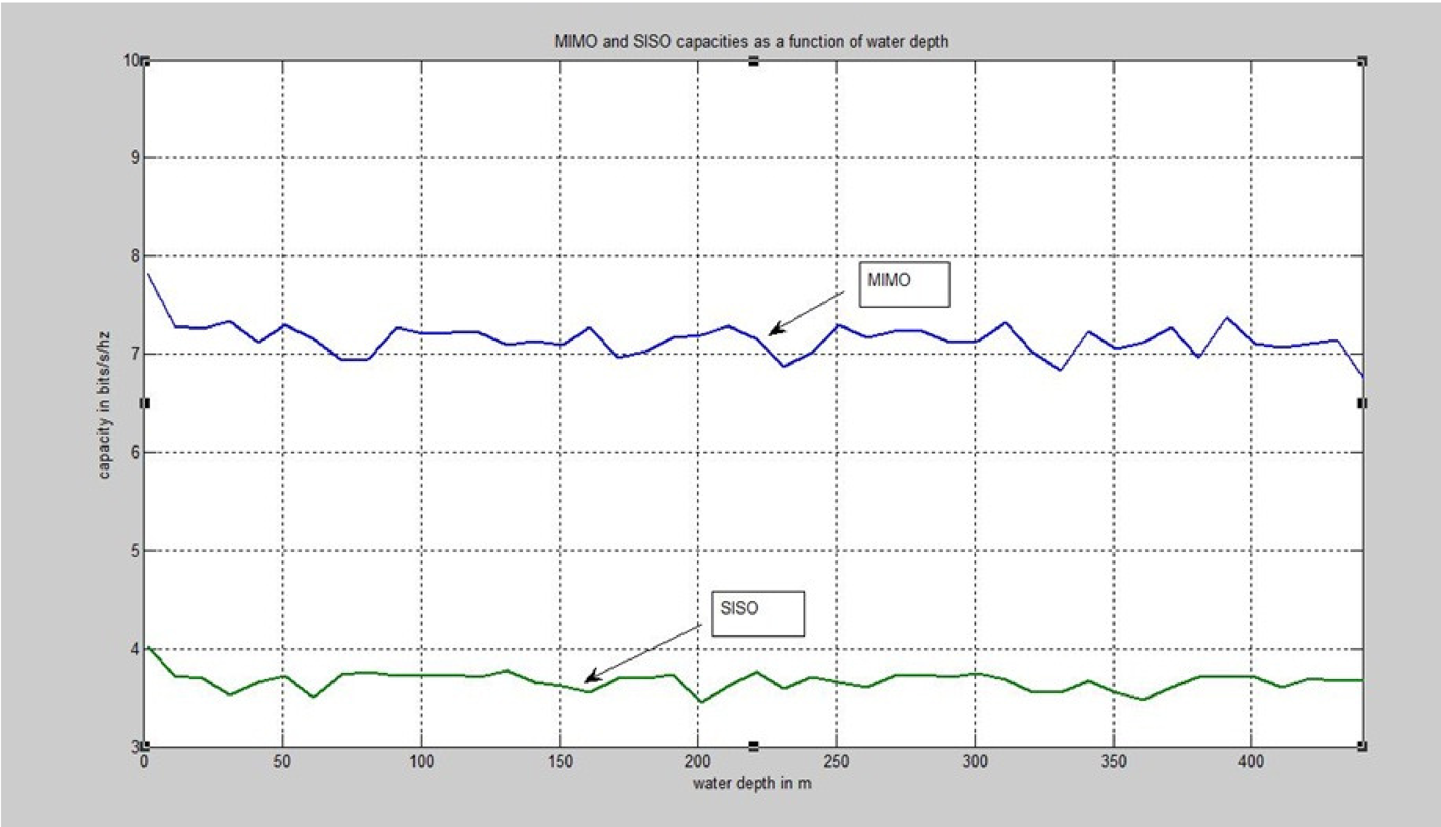

Fig.7.5. MIMO and SISO Capacities as function of water depth, *SNR* = 15dB

Discussion

1. This decrease in MIMO capacity gain with increasing depth is easily explained by the fact that MIMO capacity is strongly associated with the correlation between sub-channels which is mathematically represented by matrix determinant of $\mathbf{HH}^{\mathbf{T}}$:

   The smaller is the spatial correlation the larger is the MIMO capacity gain.
2. The lowest spatial correlation is observed for a rich multi-paths environment which occurs when the water depth of the channel is very shallow.
3. But some specific combinations of path delays gives rise to low correlation configurations which explain the presence of local maximums observed along the MIMO curve.

7.5. Relation between capacity and vertical separation of hydrophones

Fig. OUTPUT6. shows the MIMO and SISO Capacities as a function of hydrophones vertical separation (Δzt = Δzr) for a fixed SNR of 15 dB

We know that, MIMO capacity of SWA channel is a function of the correction between each one of the sub-channels linking to each of the multi sensors. As reflection interfaces (ocean-surface and ocean-bed) are located in the vertical direction relative to hydrophones, the minimum spatial correlation configurations are obtained when the hydrophone array is oriented in the vertical direction. Moreover, an easier way of ensuring uncorrelated links is to space sufficiently each of the hydrophones in the transmitter or the receiver arrays

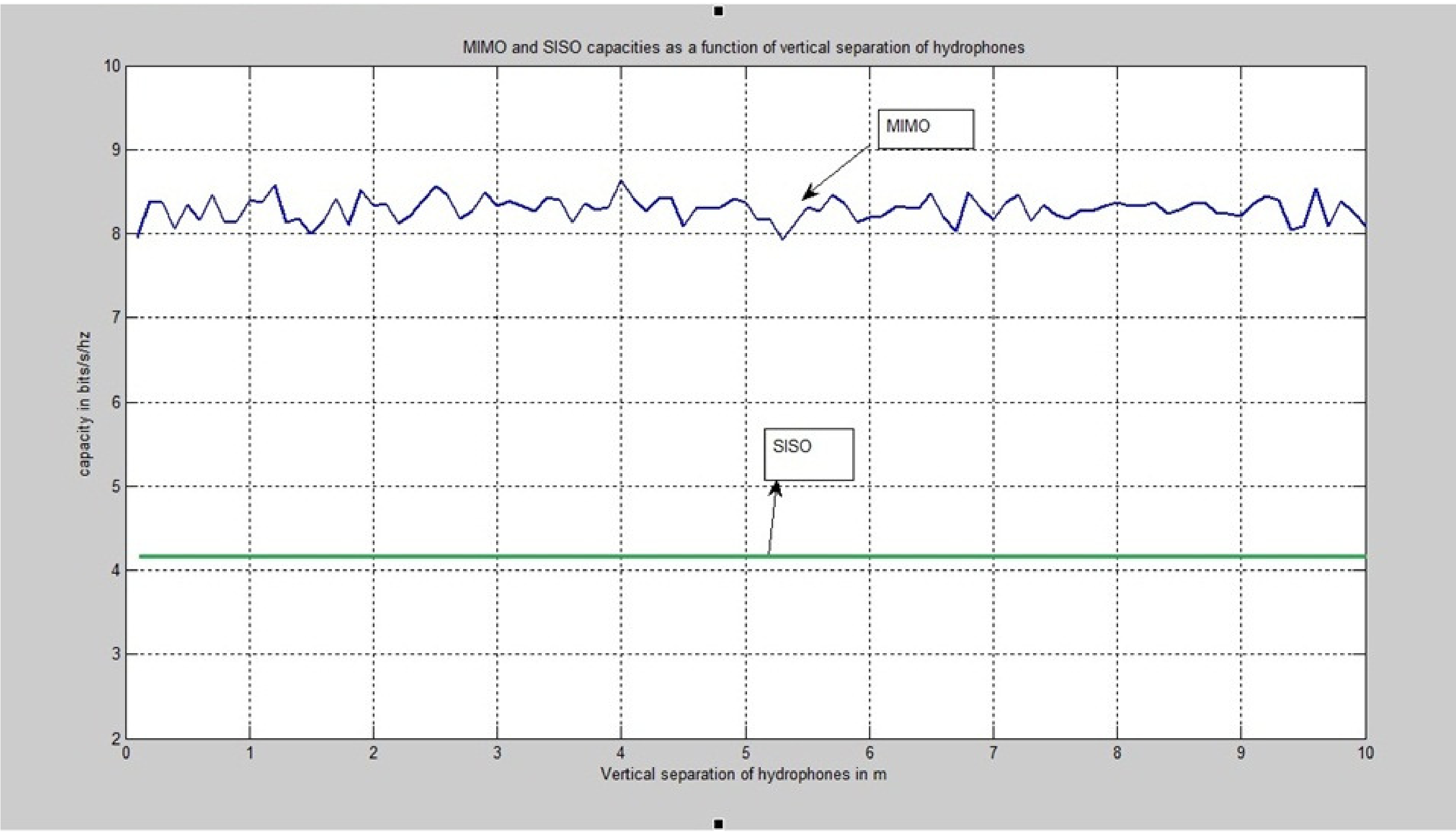

Fig. 7.6. MIMO and SISO Capacities as function of hydrophones vertical separation ($\Delta zt = \Delta zr$), SNR = 15 dB

Discussion

1. As shown in the above figure ,where MIMO capacity is plotted with varying hydrophone separation, one can observe that perfect uncorrelation is obtained when hydrophone separation is found to be greater than 0.8 m.
2. The oscillation phenomenon which is observed for large values of Δzt and Δzr results due to the phase combination of $Hmn(f)$ which is linked to the distance and causes periodic variations in the correlation ratio.
3. Furthermore it is interesting to see that low-spaced arrays lead to capacities which always remain larger than the SISO case. In fact, for the extreme value of $\Delta = 0$, MIMO SWA capacity is 4.8 b/s/Hz whereas SISO SWA capacity is 3.93 which still represents a capacity gain of 22 %.

8. CONCLUSIONS

The primary aim of this project was to quantify and predict the gain brought by MIMO technology for underwater acoustic communication. With the help of the ray-theory approach and under the assumption of shallow water environment, our project provides a model of the MIMO underwater acoustic channel taking into consideration all the under-sea dominant disturbances. A numerical evaluation of the underwater channel capacity is then used which leads to an accurate approximation of the maximum achievable data transmission rate for a given set of underwater communication parameters. Extensive simulation results for several transmission parameters and channel configuration show the expected MIMO gain is significant and the capacity increase is in the same order as that of wireless transmission. Our analysis has also demonstrated some restrictions on frequencies, communication range as well as underwater environment have to be made in order to ensure that MIMO capacity gain is maximum. More importantly, medium range transmission over shallow water channel(SWA) appears to be a dedicated system to MIMO transmission. With the above capacity based approach, our project depicts a simple means to provide an upper bound on the expected MIMO gain in the field of undersea acoustics and forms a useful tool in designing and optimizing future MIMO underwater communication system.

9.REFERENCES:

1. Capacity analysis of underwater acoustic MIMO communications by Pierre-Jean BOUVET and Alain LOUSSERT 978-1-4244-5222-4/10/$26.00 ©2010 IEEE.
2. R. S. H. Istepanian and M. Stojanovic, Underwater acoustic digital signal processing and communication systems. Kluwer Academic Pub., 2002.
3. I.F. Akyildiz, D. Pompili, and T. Melodia, "Underwater acoustic sensor networks: research challenges," Ad Hoc Network Jorunal, vol. 3, no. 3, pp. 257–279, 2005.
4. D. Gesbert, M. Shafi, D. Shiu, and P. Smith, "From theory to practice: An overview of space-time coded mimo wireless systems," IEEE J. Sel. Areas Commun., Apr. 2003.
5. A.Paulraj, A. D. Gore, R. U. Nabar, and H. Boelcskei, "An overview of MIMO communications: A key to gigabit wireless," Proceedings of the IEEE, vol. 92, no. 2, pp. 198–218, Feb. 2004.
6. D. B. Kilfoyle, J. C. Preisig, and A. B. Baggeroer, "Spatial modulation experiments in the underwater acoustic channel," IEEE J. Ocean. Eng., vol. 30, no. 2, pp. 406–415, Apr. 2005.
7. B. Li, J. Huang, S. Zhou, K. Ball, M. Stojanovic, L. Freitag, and P. Willett, "MIMO-OFDM for high rate underwater acoustic communications," IEEE J. Ocean. Eng., vol. 34, no. 4, pp. 634–644, 2009.
8. T. J. Hayward and T. C. Yang, "Underwater acoustic communication channel capacity: A simulation study," in Proceedings of High Frequency Ocean Acoustics Conference, vol. 728, 2004, pp. 114–121.

9. M. Stojanovic, “On the relationship between capacity and distance in an underwater acoustic communication channell,” ACM SIGMOBILE Mobile comput. and Comm. Review (M2CR), vol. 11, pp. 34–43, Oct. 2007.

10. T. J. Hayward and T. C. Yang, “Single- and multi-channel underwater acoustic communication channel capacity: A computational study,” Journal of the Acoustical Society of America, vol. 122, no. 3, pp. 1652– 1661, Sep. 2007.

11. M. A. Chitre, “A high-frequency warm shallow water acoustic communications channel model and measurements,” Journal of the Acoustical Society of America, vol. 5, no. 122, pp. 2580–2586, 2007.